

# Improving Plasticity in Non-stationary Reinforcement Learning with Evidential Proximal Policy Optimization

Abdullah Akgül, Gulcin Baykal, Manuel Haußmann, Melih Kandemir

{akgul,baykalg,haussmann,kandemir}@imada.sdu.dk

Department of Mathematics and Computer Science, University of Southern Denmark, Denmark

## Abstract

On-policy reinforcement learning algorithms use the most recently learned policy to interact with the environment and update it using the latest gathered trajectories, making them well-suited for adapting to non-stationary environments where dynamics change over time. However, previous studies show that they struggle to maintain plasticity—the ability of neural networks to adjust their synaptic connections—with overfitting identified as the primary cause. To address this, we present the first application of evidential learning in an on-policy reinforcement learning setting: *Evidential Proximal Policy Optimization (EPPO)*. EPPO incorporates all sources of error in the critic network’s approximation—i.e., the baseline function in advantage calculation—by modeling the epistemic and aleatoric uncertainty contributions to the approximation’s total variance. We achieve this by using an evidential neural network, which serves as a regularizer to prevent overfitting. The resulting probabilistic interpretation of the advantage function enables optimistic exploration, thus maintaining the plasticity. Through experiments on non-stationary continuous control tasks, where the environment dynamics change at regular intervals, we demonstrate that EPPO outperforms state-of-the-art on-policy reinforcement learning variants in both task-specific and overall return.

## 1 Introduction

On-policy algorithms, such as Proximal Policy Optimization (PPO) (Schulman et al., 2017), update the learned policy using data collected from their most recent interactions with the environment. This makes them particularly applicable for non-stationary environments where the state transition dynamics or reward function change over time. These changes often appear as a sequence of tasks, requiring the agent to adapt continually. Many real-world applications are naturally non-stationary (Hadsell et al., 2020). Consider a robotic arm experiencing wear and tear, leading to changes in the ability of its joints to apply torque, or an autonomous robot navigating rough terrain with varying ground conditions that affect friction. In such environments, an agent can maintain high performance only if it keeps modifying its policy throughout its whole life cycle to adapt to the continual changes that affect its actuators and the surrounding environment.

Plasticity refers to the ability of a neural network to change its wiring in response to new observations that appear at late stages of an online learning regime. It is an essential property in designing adaptive systems for non-stationary environments. Many of the existing deep reinforcement algorithms suffer from the problem of the *loss of plasticity* under non-stationarity. This observation comprises both PPO variants (Dohare et al., 2021; 2023; 2024; Moalla et al., 2024) and other model families (Kumar et al., 2021; Lyle et al., 2022; Nikishin et al., 2022; Lyle et al., 2023; Abbas et al., 2023; Kumar et al., 2025). We introduce a novel solution to this deep-rooted problem that sets a severe bottleneck for building autonomous systems using deep reinforcement learning approaches.

Existing research tends to attribute the loss of plasticity to various factors. [Dohare et al. \(2021; 2023; 2024\)](#) treat the loss of plasticity in PPO as an optimization issue. Therefore, [Dohare et al. \(2021; 2024\)](#) propose a continual backpropagation algorithm to mitigate decaying plasticity while [Dohare et al. \(2023\)](#) propose to use a non-stationary adaptation of the Adam optimizer ([Kingma & Ba, 2015](#)) where the exponential decay rates for the moment estimates are equal ([Lyle et al., 2023](#)). Recently, [Moalla et al. \(2024\)](#) relate PPO’s loss of plasticity to feature rank deterioration and capacity loss, showing that non-stationarity worsens these effects. They attempt to solve the problem by regularizing the representation dynamics of the policy by a new term in the training objective. They name their method Proximal Feature Optimization (PFO). We show in experiments that this method improves the plasticity of the vanilla PPO only to a certain degree.

The primary challenge in maintaining plasticity is the difficulty of protecting the model from overfitting to the past observations ([Nikishin et al., 2022](#)). We observe the plasticity preserving methods developed for PPO miss to identify overfitting as the root cause of the problem. We propose a new method called *Evidential Proximal Policy Optimization (EPPO)* that approaches the problem from an overfitting perspective. We summarize our contributions as follows:

- (i) EPPO addresses the overfitting problem using probabilistic inference methods observed to be powerful in various deep learning applications but not yet employed to overcome the loss of plasticity. We take evidential deep learning ([Sensoy et al., 2018](#)) as a starting point and apply it for the first time to uncertainty-aware modeling of the value function in a PPO learning pipeline. We name this approach as *evidential value learning*. Since value functions have a range on the real line, we build on an established extension of evidential deep learning to regression ([Amiri et al., 2020](#)).
- (ii) We use evidential value learning to develop three ways to construct a probabilistic extension of the *generalized advantage estimator* ([Schulman et al., 2016](#)). We show in our experiments that performing optimistic exploration based on the probabilistic advantage estimators brings a consistent performance boost.
- (iii) We introduce two new experiment designs tailored for the evaluation of deep reinforcement learning algorithms developed for the continuous control of locomotors under non-stationary dynamics. Our design improves those of [Dohare et al. \(2021; 2024\)](#); [Al-Shedivat et al. \(2018\)](#). We benchmark EPPO against two state-of-the-art on-policy learning variants on these new setups and observe it to outperform them in far majority of the cases.

## 2 Preliminaries

### 2.1 Reinforcement Learning

**Background and Notation.** We define an infinite-horizon Markov Decision Process (MDP) as a tuple  $\mathcal{M} \triangleq \langle \mathcal{S}, \mathcal{A}, P, r, \rho_0, \gamma \rangle$  where  $\mathcal{S}$  represents the state space and  $\mathcal{A}$  denotes the action space. The state transition distribution is defined as  $P : \mathcal{S} \times \mathcal{A} \times \Delta(\mathcal{S}) \rightarrow [0, 1]$ , where  $\Delta(\mathcal{S})$  denotes the probability simplex over the state space. We assume a deterministic reward function  $r : \mathcal{S} \times \mathcal{A} \rightarrow \mathbb{R}$  without loss of generality of our findings. The MDP includes an initial state distribution  $\rho_0 \in \Delta(\mathcal{S})$  and a discount factor  $\gamma \in (0, 1)$ . Let  $\pi$  denote a stochastic policy  $\pi : \mathcal{S} \times \Delta(\mathcal{A}) \rightarrow [0, 1]$ . We use the following standard definitions of the action-value function  $Q^\pi$ , the value function  $V^\pi$ , and the advantage function  $A^\pi$ :

$$Q^\pi(s_t, a_t) \triangleq \mathbb{E}_{a_{t+1:\infty}}^{s_{t+1:\infty}} \left[ \sum_{l=0}^{\infty} \gamma^l r_{t+l} \right], \quad V^\pi(s_t) \triangleq \mathbb{E}_{a_{t:\infty}}^{s_{t+1:\infty}} \left[ \sum_{l=0}^{\infty} \gamma^l r_{t+l} \right],$$

$$A^\pi(s_t, a_t) \triangleq Q^\pi(s_t, a_t) - V^\pi(s_t),$$

where expectations are taken over trajectories following the policy  $\pi$ , and  $r_{t+l} \triangleq r(s_{t+l}, a_{t+l})$ . The colon notation  $a : b$  refers to the inclusive range  $(a, a + 1, \dots, b)$ . We denote the return  $G_t \triangleq \sum_{l=0}^{\infty} \gamma^l r_{t+l}$  as the discounted sum of rewards.

**On-policy Reinforcement Learning** approaches (Williams, 1992; Schulman et al., 2015; 2017) offer several advantages. *i)* On-policy methods avoid overestimation and underestimation biases because they do not use bootstrapping and evaluate only their own actions (Sutton & Barto, 1998). *ii)* On-policy algorithms demonstrate robust and stable training regimes since they update their policy using the most recently collected data (Schulman et al., 2015). *iii)* Providing performance guarantees for on-policy algorithms is simpler because average policy improvement is sufficient (Kakade & Langford, 2002). *iv)* On-policy algorithms are easy to implement and integrate, as they use the same policy for exploration and exploitation (Schulman et al., 2016). These advantages make them a natural choice for various applications, such as robotics (Lopes et al., 2018; Melo & Máximo, 2019), and fine-tuning large language models (Achiam et al., 2023; Touvron et al., 2023; Christiano et al., 2017; Bai et al., 2022b; Zheng et al., 2023).

The commonplace choice for an on-policy algorithm is PPO (Schulman et al., 2017). PPO is a policy gradient algorithm where the policy is updated with a surrogate objective which regularizes the policy updates to be in the trust region. We follow the established practice and adopt the clipped objective as the surrogate function. PPO updates its policy  $\pi_\theta$  parametrized with  $\theta \in \Theta$ :

$$\mathcal{L}_{\text{clip}}(\theta) = \mathbb{E}_{(s,a) \sim \pi_{\text{old}}} \left[ \min \left( \frac{\pi_\theta(a|s)}{\pi_{\text{old}}(a|s)} \hat{A}^{\pi_{\text{old}}}(s, a), \text{clip} \left( \frac{\pi_\theta(a|s)}{\pi_{\text{old}}(a|s)}, 1 - \epsilon, 1 + \epsilon \right) \hat{A}^{\pi_{\text{old}}}(s, a) \right) \right],$$

where  $\hat{A}^{\pi_{\text{old}}}(s, a)$  is an estimate of the advantage function, and  $\text{clip}(\frac{\pi_\theta(a|s)}{\pi_{\text{old}}(a|s)}, 1 - \epsilon, 1 + \epsilon)$  bounds the probability ratio to within the range of  $[1 - \epsilon, 1 + \epsilon]$  for  $\epsilon > 0$ . PPO learns a value function approximation  $V_\phi$ , parametrized with  $\phi \in \Phi$  with squared error loss  $\mathcal{L}_{\text{VF}}(\phi) = \mathbb{E}_{s_t} [(V_\phi(s_t) - G_t)^2]$ . The learned  $V_\phi$  is then used to compute advantage estimates, guiding policy updates for more stable and efficient learning.

**Generalized Advantage Estimation (GAE)** (Schulman et al., 2016) is a technique for computing advantage estimates, helping to balance the bias-variance trade-off by reducing variance and introducing bias. GAE constructs the advantage function using a weighted sum of multi-step temporal difference errors. The temporal difference residual at time step  $t$  is  $\delta_t \triangleq r_t + \gamma V_\phi(s_{t+1}) - V_\phi(s_t)$ . The GAE estimate is the exponentially weighted sum of temporal difference residuals:

$$\hat{A}_t^{\text{GAE}(\lambda), \pi} = \sum_{l=0}^{\infty} (\gamma \lambda)^l \delta_{t+l}, \quad (1)$$

where  $\lambda \in [0, 1]$  is a hyperparameter that controls the bias-variance trade-off. GAE provides a flexible mechanism for estimating advantages, enabling reinforcement learning algorithms to achieve improved stability and faster convergence (Schulman et al., 2015; 2017).

**Non-stationary Reinforcement Learning.** Various methods in the literature address the challenges of learning in non-stationarity through diverse settings (Khetarpal et al., 2020), such as meta-learning (Al-Shedivat et al., 2018; Berseth et al., 2021; Bing et al., 2023) and continual learning (Rusu et al., 2016; Kirkpatrick et al., 2017; Traoré et al., 2019; Kaplanis et al., 2019). While these have shown promising result, most of them primarily focus on mitigating catastrophic forgetting—often at the cost of plasticity. Methods that strongly constrain updates to preserve past knowledge may hinder the agent’s ability to adapt to significant environmental changes, which is crucial in non-stationarity. Therefore, we focus on preserving plasticity, which is essential for effective long-term adaptation with minimal regret.

## 2.2 Evidential Deep Learning

Bayesian inference (Bishop, 2006; Gelman et al., 2013) infers a posterior over parameters, given a likelihood and data-independent prior. Evidential deep learning (Sensoy et al., 2018) modifies this by instead learning an evidential, i.e., data-dependent prior, whose parameters are usually inferred by a neural net. Choosing this prior to be conjugate to the likelihood provides an analytically tractable

marginal likelihood as the objective, which can be optimized via gradient descent. Marginal likelihood optimization is also known as *Type II Maximum Likelihood* or *Empirical Bayes* (Efron, 2012).

Amini et al. (2020) extends evidential deep learning (Sensoy et al., 2018) to regression. We build our solution on their formulation as value function approximation, which is a regression problem. They assume a target  $y$  with features  $\mathbf{x}$  to be normally distributed, whose mean  $\mu$  and variance  $\sigma^2$  follow an evidential prior Normal Inverse-Gamma ( $\mathcal{NIG}$ ) distribution:

$$\begin{aligned} (\mu, \sigma^2) | \mathbf{m}(\mathbf{x}) &\sim \mathcal{NIG}(\mu, \sigma^2 | \omega(\mathbf{x}), \nu(\mathbf{x}), \alpha(\mathbf{x}), \beta(\mathbf{x})) \\ &= \mathcal{N}(\mu | \omega(\mathbf{x}), \sigma^2 \nu(\mathbf{x})^{-1}) \text{InvGam}(\sigma^2 | \alpha(\mathbf{x}), \beta(\mathbf{x})), \end{aligned}$$

where the parameters are parameterized by a neural network with weights  $\phi$ . Throughout the paper, we suppress the dependence on  $\phi$  and  $\mathbf{x}$  from the notation, e.g.,  $\omega = \omega_\phi(\mathbf{x})$ , and refer to them jointly as  $\mathbf{m} \triangleq \mathbf{m}_\phi = (\omega, \nu, \alpha, \beta)$ . Due to its conjugacy to the normal likelihood  $p(y | \mu, \sigma^2) = \mathcal{N}(y | \mu, \sigma^2)$ , its posterior and marginal likelihood are analytically tractable. This marginal is well-known to be Student-t distributed:

$$y | \mathbf{m} \sim \text{St}\left(y | \omega, \frac{\beta(1-\nu)}{\nu\alpha}, 2\alpha\right).$$

The parameters of this distribution can be optimized by Type II Maximum Likelihood, i.e., log minimizing objective is given as

$$\mathcal{L}_{\text{NLL}}(\mathbf{m}) = \frac{1}{2} \log\left(\frac{\pi}{\nu}\right) - \alpha \log(\Omega) + \left(\alpha + \frac{1}{2}\right) \log\left((y - \omega)^2 \nu + \Omega\right) + \log\left(\frac{\Gamma(\alpha)}{\Gamma\left(\alpha + \frac{1}{2}\right)}\right), \quad (2)$$

where  $\Omega = 2\beta(1 + \nu)$  and  $\Gamma(\cdot)$  is the Gamma function. See Section 6 for the posterior and additional derivations.

**Evidential Deep Learning in Deep Reinforcement Learning.** Evidential deep learning has been extensively used in numerous machine learning frameworks and practical tasks (Gao et al., 2024). It has also been integrated into deep reinforcement learning for recommendation systems to provide uncertainty-aware recommendations (Wang et al., 2024), modeling policy network uncertainty to guide evidence-based exploration in behavioral analysis (Wang et al., 2023), incorporating uncertainty measures as rewards for decision-making in opinion inference tasks (Zhao et al., 2019), and calibrating prediction risk in safety-critical vision tasks through fine-grained reward optimization (Yang et al., 2024). Evidential deep learning is commonly used in reinforcement learning to leverage uncertainty for exploration or anti-exploration strategies. However, we aim to use it for modeling uncertainty in value function estimates, which also enables confidence-based exploration.

### 3 Method

We introduce a new method that adapts the evidential approach to learning a distribution over the value function  $V(s_t)$  by introducing a new concept we refer to as *Evidential Value Learning*. The inferred distribution in turn induces another distribution over the GAE, which provides a guiding signal for both regularization and optimistic exploration.

#### 3.1 Evidential Value Learning

We adopt Amini et al. (2020)’s approach to perform evidential value function learning in an evidential way. We assume our value function estimates  $V(s_t)$  to be normally distributed with unknown mean  $\mu$  and variance  $\sigma^2$  which are jointly  $\mathcal{NIG}$  distributed. We shorten the notation to  $V_t = V(s_t)$  whenever the relation is clear from the context. Naïvely following Amini et al. (2020)’s method would result in training instabilities similar to those found by Meinert et al. (2023) for regular supervised regression. Instead of following their non-Bayesian heuristic, we propose instead to use hyperpriors to regularize and stabilize the objective.

We therefore introduce hyperpriors on each of the four evidential parameters, giving us

$$\begin{aligned}
\omega(s) &\sim \mathcal{N}(\omega(s) | \mu_\omega^0, (\sigma_\omega^0)^2), \\
\nu(s) &\sim \mathcal{Gam}(\nu(s) | \alpha_\nu^0, \beta_\nu^0), \\
\alpha(s) &\sim \mathcal{Gam}(\alpha(s) | \alpha_\alpha^0, \beta_\alpha^0), \\
\beta(s) &\sim \mathcal{Gam}(\beta(s) | \alpha_\beta^0, \beta_\beta^0), \\
\sigma^2 &\sim \text{InvGam}(\sigma^2 | \alpha(s), \beta(s)), \\
\mu | \sigma^2 &\sim \mathcal{N}(\mu | \omega(s), \sigma^2 \nu(s)^{-1}), \\
V | \mu, \sigma^2 &\sim \mathcal{N}(V | \mu, \sigma^2),
\end{aligned}$$

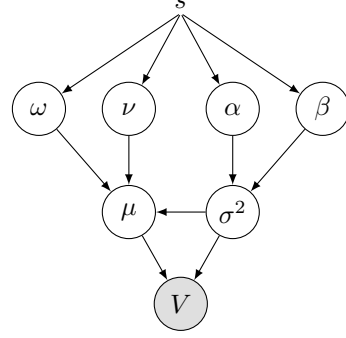


Figure 1: Plate diagram of our evidential value learning model.

where  $\mathcal{Gam}(\cdot)$  is the Gamma distribution,  $\mu_\omega^0, \dots, \beta_\beta^0$  are fixed hyperparameters, and we suppress the time dependence from the notation. We choose hyperpriors to provide relatively flat, uninformative priors and keep them constant for all experiments. As before, we suppress the dependency on  $s$  from the notation, e.g.,  $\omega = \omega(s)$ , and combine the evidential parameters into  $\mathbf{m} = (\omega, \nu, \alpha, \beta)$ . Marginalizing over  $(\mu, \sigma^2)$  yields

$$p(V, \mathbf{m}) = \int p(V | \mu, \sigma^2) p(\mu, \sigma^2 | \mathbf{m}) d(\mu, \sigma^2) p(\mathbf{m}) = p(V | \mathbf{m}) p(\mathbf{m}),$$

where  $p(V | \mathbf{m})$  is a Student-t distribution parameterized as in Section 2.2. The hyperprior  $p(\mathbf{m})$  plays the role of a regularizer in the logarithm of the joint. The training objective then becomes  $\mathcal{L}_{\text{EVL}}(\mathbf{m}) = \mathcal{L}_{\text{NLL}}(\mathbf{m}) - \xi \log p(\mathbf{m})$ , where  $\xi \geq 0$  is a regularization coefficient. We summarize the model as a plate diagram in Figure 1.

The mean and variance of the values  $V$  remain analytically tractable and are given as

$$\mathbb{E}_{V | \mathbf{m}} [V] = \mathbb{E}_{(\mu, \sigma^2) | \mathbf{m}} [\mathbb{E}_{V | \mu, \sigma^2} [V]] = \mathbb{E}_{(\mu, \sigma^2) | \mathbf{m}} [\mu] = \omega,$$

and

$$\begin{aligned}
\text{var}_{V | \mathbf{m}} [V] &= \mathbb{E}_{(\mu, \sigma^2) | \mathbf{m}} [\text{var}_{V | \mu, \sigma^2} [V]] + \text{var}_{(\mu, \sigma^2) | \mathbf{m}} [\mathbb{E}_{V | \mu, \sigma^2} [V]] \\
&= \mathbb{E}_{(\mu, \sigma^2) | \mathbf{m}} [\sigma^2] + \text{var}_{(\mu, \sigma^2) | \mathbf{m}} [\mu] \\
&= \frac{\beta}{\alpha - 1} + \frac{\beta}{\nu(\alpha - 1)} = \frac{\beta}{\alpha - 1} \left( 1 + \frac{1}{\nu} \right),
\end{aligned}$$

where we assume  $\alpha > 1$ ,<sup>1</sup> and the first equality is due to the law of total variance splitting the marginal variance into aleatoric and epistemic uncertainty. Reliance on  $\text{var}_{y | \mathbf{m}} [y]$  therefore provides us with a principled way of incorporating both irreducible uncertainty due to the environment as well as reducible uncertainty due to our current model approximation into EPPO.

**Distributional Reinforcement Learning.** Evidential value learning belongs to a broader research field that incorporates distributional information into the reinforcement learning model, which can be roughly split into two sub-fields. The first aims to account for aleatoric uncertainty caused by the inherent stochasticity of the environment. It’s focus is on accurately modeling the resulting distribution over the returns  $G_t$ , e.g., to infer risk-averse policies (Keramati et al., 2020). See Bellemare et al. (2023) for a recent textbook introduction. The other’s focus is on accounting for epistemic uncertainty inherent in the inference of a value function, usually relying on methods from Bayesian inference (Ghavamzadeh et al., 2015; Luis et al., 2024), e.g., to use it as a guide for exploration (e.g., Deisenroth & Rasmussen, 2011; Osband et al., 2019). Evidential value learning is relative to this second area of research, by using an evidential model over the value function to induce a distribution over an advantage function that incorporates aleatoric and epistemic uncertainty for regularization and optimistic exploration.

<sup>1</sup>We enforce this condition by adding a constant shift to the neural network’s output.

### 3.2 Optimistic Exploration via Upper Confidence Bound

Our distribution  $p(V|\mathbf{m})$  yields a probabilistic GAE which we denote as  $\hat{A}_t^{\text{GAE}}$ . Such a probabilistic modeling of the value function enables the construction of an upper confidence bound (UCB) on the advantage estimator:

$$\hat{A}_t^{\text{UCB}} = \mathbb{E} \left[ \hat{A}_t^{\text{GAE}} \right] + \kappa \sqrt{\text{var} \left[ \hat{A}_t^{\text{GAE}} \right]}, \quad (3)$$

where  $\kappa \geq 0$  controls the confidence radius, and  $\text{var} \left[ \hat{A}_t^{\text{GAE}} \right]$  represents the variance estimate of GAE. We introduce three variants for applying UCB.

**Pure exploitation: EPPO<sub>mean</sub>.** Since the mean of the temporal difference  $\mathbb{E} [\delta_t] = r_t + \gamma \mathbb{E} [V_t]$  is tractable,  $\mathbb{E} [\hat{A}_t^{\text{GAE}(\lambda, \pi)}] = \sum_{l=0}^{\infty} (\gamma \lambda)^l \mathbb{E} [\delta_{t+l}]$  is also tractable due to the linearity of expectations. Relying solely on this posterior mean, i.e., by choosing  $\kappa = 0$  in (3), we no longer incorporate additional distributional information and have a purely exploitative estimator without optimistic exploration.

**Correlated exploration: EPPO<sub>cor</sub>.** We can derive the variance of  $\hat{A}_t$  by focusing on its definition as the exponentially-weighted average of the  $k$ -step estimators  $\hat{A}_t^{(k)} = -V_t + \gamma^k V_{t+k} + \sum_{l=0}^{k-1} \gamma^l r_{t+l}$ . As the rewards are deterministic in our setup and have zero variance, we combine them into a generic constant term and obtain

$$\begin{aligned} \hat{A}_t^{\text{GAE}} &\triangleq (1 - \lambda) \sum_{l=1}^{\infty} \lambda^{l-1} \hat{A}_t^{(l)} = (1 - \lambda) \left( -V_t \sum_{l=0}^{\infty} \lambda^l + \sum_{l=1}^{\infty} \gamma^l \lambda^{l-1} V_{t+l} \right) + \text{const} \\ &= -V_t + \frac{1 - \lambda}{\lambda} \sum_{l=1}^{\infty} (\gamma \lambda)^l V_{t+l} + \text{const}. \end{aligned}$$

Given the conditional independence of the states, the resulting variance is

$$\text{var} \left[ \hat{A}_t^{\text{GAE}} \right] = \text{var} [V_t] + \left( \frac{1 - \lambda}{\lambda} \right)^2 \sum_{l=1}^{\infty} (\gamma \lambda)^{2l} \text{var} [V_{t+l}]. \quad (4)$$

We use this variance to construct the UCB in Equation (3) with  $\kappa > 0$ . We refer to this estimator as EPPO<sub>cor</sub> in the experiments.

**Uncorrelated exploration: EPPO<sub>ind</sub>.** We also consider the case where the  $k$ -step estimators  $\hat{A}_t^{(k)}$  are assumed to be independent of each other. We then build the overall variance as the exponentially weighted sum of the individual  $k$ -step estimators. It can easily be shown (see Section 6.2) that the resulting variance approximation is

$$\text{var} \left[ \hat{A}_t^{\text{GAE}} \right] \approx \frac{1 - \lambda}{1 + \lambda} \text{var} [V_t] + \left( \frac{1 - \lambda}{\lambda} \right)^2 \sum_{l=1}^{\infty} (\gamma \lambda)^{2l} \text{var} [V_{t+l}], \quad (5)$$

i.e., the influence of the current value variance is down-scaled by a factor  $(1 - \lambda)/(1 + \lambda) < 1$  relative to the future time steps in EPPO<sub>ind</sub> compared to EPPO<sub>cor</sub>. We use the variance estimate in Equation (5) to construct the UCB in Equation (3) with  $\kappa > 0$ .

## 4 Experiments

Our experiments analyze the performance of state-of-the-art and EPPO variants in non-stationary environments where dynamics change over time. To this end, we define tasks as short time intervals and introduce changes in the environment dynamics. For example, these modifications can involve adjusting the friction coefficient of the floor in a locomotion task. The expected behavior of the agent



Table 1: *Results Summary*. The average scores and ranks across experiments are computed based on the Area Under the Learning Curve (AULC) and Final Return. EPPO algorithms outperform others in adapting to both individual tasks and the overall set of tasks.

Experiment		AULC					FINAL RETURN				
		PPO	PFO	EPPO <sub>mean</sub>	EPPO <sub>cor</sub>	EPPO <sub>ind</sub>	PPO	PFO	EPPO <sub>mean</sub>	EPPO <sub>cor</sub>	EPPO <sub>ind</sub>
Slippery	AVERAGE (↑)	2391	2256	2586	<b>2982</b>	2919	2448	2336	2707	<b>3150</b>	3065
	RANK (↓)	4.3	3.8	3.5	2.0	<b>1.5</b>	4.3	4.3	3.3	1.8	<b>1.5</b>
Paralysis	AVERAGE (↑)	2199	2082	2623	2763	<b>2812</b>	2386	2256	2849	3011	<b>3054</b>
	RANK (↓)	4.0	4.2	2.8	2.2	<b>1.8</b>	3.9	4.3	2.8	2.2	<b>1.8</b>
Overall	AVERAGE (↑)	2254	2132	2612	2826	<b>2842</b>	2404	2279	2808	3050	<b>3057</b>
	RANK (↓)	4.1	4.1	3.0	2.0	<b>1.7</b>	4.0	4.3	2.9	2.1	<b>1.7</b>

is to maintain plasticity, meaning that it adapts to all tasks as quickly as possible while maximizing the overall return during learning. We adopt the `Ant` and `HalfCheetah` environments using the ‘v5’ versions of MuJoCo environments (Todorov et al., 2012), as these tasks are stable and do not reward the agent simply for maintaining stability. For further details on the experimental pipeline and hyperparameters, see Section 7.

We evaluate the model performance using two scores: (i) *Area Under Learning Curve (AULC)*: The average return computed throughout training. (ii) *Final Return*: The average return computed at the final steps of training for each task. AULC indicates how much reward is collected throughout the entire training process and how quickly a model converges to its final performance. A higher AULC suggests greater adaptation ability during training, assuming other factors remain equal. The final return measures an agent’s ability to fit to each task. A higher final return score reflects better performance on a specific task. These metrics evaluate an agent’s adaptation performance, plasticity, and susceptibility to overfitting.

We compare EPPO algorithms with the following models: (i) *PPO* (Schulman et al., 2017): A widely employed on-policy reinforcement learning algorithm for many problems, used as the foundation for EPPO. (ii) *PFO* (Moalla et al., 2024): A state-of-the-art PPO variant that addresses the plasticity problem by extending its trust region to the feature space.

#### 4.1 Experiments on Slippery Environments

Inspired by Dohare et al. (2021; 2024), we construct a non-stationary environment by varying the friction coefficient of the floor in locomotion tasks using the `Ant` and `HalfCheetah` environments. We induce non-stationarity to the environments by changing friction once in every 500 000 steps. We implement two strategies for these changes: *decreasing*, where friction starts at its maximum value and gradually decreases, and *increasing*, where friction starts at its minimum value and gradually increases. This setup ensures that agents encounter non-stationarity in both increasing and decreasing friction scenarios. The minimum friction is set to 0.5 and the maximum to 4.0, based on the feasibility of solving the tasks—extreme friction values may make movement too difficult due to excessive slipping or an inability to move forward. We define 15 tasks by changing the friction by a positive or negative offset of 0.25.

#### 4.2 Experiments on Paralysis Environments

We design a new set of non-stationarity experiments by dynamically altering the torque capabilities of the leg joints in the `Ant` and `HalfCheetah` environments, inspired by Al-Shedivat et al. (2018). We generate six torque modification schemes for `Ant` and four for `HalfCheetah`. In each scheme, we select specific joints and progressively reduce their torque capability until they become fully paralyzed. Then, we gradually restore their functionality, returning to the fully operational state. This results in a sequence of nine tasks, where each joint either loses or regains 25% of its torque capacity in each step, following the pattern: [100, 75, 50, 25, 0, 25, 50, 75, 100].

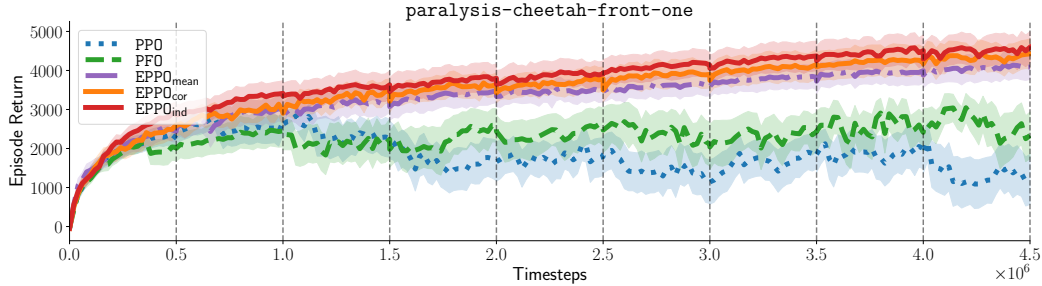


Figure 2: Learning curves for the `paralysis` experiment in the `HalfCheetah` environment with the `front-one` setting. The curves show the mean returns across ten evaluation episodes and ten random seeds. The shaded area gives one standard error around the mean.

### 4.3 Results and Discussion

We summarize all the experiments in Table 1 and provide the detailed results of the individual experiments in Tables 4 to 5. Figure 2 visualizes the episode return for one experiment throughout the changing tasks, demonstrating both the quantitative and qualitative performance difference between EPPO variations and our baselines. The remaining episode return curves are provided in Figures 3 to 5 in the appendix. Our experimental findings are as follows:

- (i) *Evidential value learning mitigates overfitting.* All EPPO variants achieve better task adaptation than the baselines, as reflected in the final return scores. The regularization scheme in evidential value learning prevents the model from overfitting to specific tasks, thanks to the probabilistic modeling of the value function.
- (ii) *Evidential value learning accelerates convergence and improves training stability while preserving plasticity.* Evidential value learning learns more efficiently and reaches final performance faster, as evident from the AULC scores. By maintaining flexibility in the value function throughout training, evidential value learning reduces loss of plasticity.
- (iii) *Optimistic exploration boosts performance.* EPPO variants with optimistic exploration outperform the baselines across both metrics, including their exploitation-focused counterpart.
- (iv)  $\text{EPPO}_{\text{ind}}$  *improves over*  $\text{EPPO}_{\text{cor}}$ . This is because  $\text{EPPO}_{\text{ind}}$  explores in a more myopic way.

## 5 Conclusion

EPPO addresses the overfitting problem in on-policy reinforcement learning algorithms, which we identify as the main cause of the loss of plasticity issue. We tackle this by incorporating evidential learning as a form of regularization. The resulting flexible probabilistic framework facilitates optimistic exploration by considering all sources of uncertainty. Through extensive evaluation in various non-stationary environments, we demonstrate the effectiveness of all EPPO variants in reducing overfitting while maintaining plasticity.

Our algorithmic framework extends beyond on-policy reinforcement learning and can benefit both off-policy and offline settings. Evidential value learning and its probabilistic exploration scheme could enhance off-policy reinforcement learning (Lillicrap et al., 2015; Fujimoto et al., 2018; Haarnoja et al., 2018). In offline reinforcement learning, evidential value learning might support uncertainty-driven methods in both model-free (An et al., 2021; Bai et al., 2022a) and model-based (Yu et al., 2020; Sun et al., 2023; Akgül et al., 2024) approaches, which apply pessimistic value iteration (Jin et al., 2021).

**Limitations.** The choice of the hyperprior and the regularization coefficient ( $\xi$ ) has an impact on the performance of the EPPO variants. Additionally, the confidence radius ( $\kappa$ ) influences the performance of the optimistic exploration variants of EPPO.



---

## References

- Zaheer Abbas, Rosie Zhao, Joseph Modayil, Adam White, and Marlos C. Machado. Loss of plasticity in continual deep reinforcement learning. In *Proceedings of The 2nd Conference on Lifelong Learning Agents*, 2023.
- Josh Achiam, Steven Adler, Sandhini Agarwal, Lama Ahmad, Ilge Akkaya, Florencia Leoni Aleman, Diogo Almeida, Janko Altenschmidt, Sam Altman, Shyamal Anadkat, et al. GPT-4 technical report. *arXiv preprint arXiv:2303.08774*, 2023.
- Abdullah Akgül, Manuel Haussmann, and Melih Kandemir. Deterministic uncertainty propagation for improved model-based offline reinforcement learning. In *Advances in Neural Information Processing Systems*, 2024.
- Maruan Al-Shedivat, Trapit Bansal, Yuri Burda, Ilya Sutskever, Igor Mordatch, and Pieter Abbeel. Continuous adaptation via meta-learning in nonstationary and competitive environments. In *International Conference on Learning Representations*, 2018.
- Alexander Amini, Wilko Schwarting, Ava Soleimany, and Daniela Rus. Deep evidential regression. In *Advances in Neural Information Processing Systems*, 2020.
- Gaon An, Seungyong Moon, Jang-Hyun Kim, and Hyun Oh Song. Uncertainty-based offline reinforcement learning with diversified Q-ensemble. In *Advances in Neural Information Processing Systems*, 2021.
- Jimmy Lei Ba, Jamie Ryan Kiros, and Geoffrey E Hinton. Layer normalization. *arXiv preprint arXiv:1607.06450*, 2016.
- Chenjia Bai, Lingxiao Wang, Zhuoran Yang, Zhihong Deng, Animesh Garg, Peng Liu, and Zhao-ran Wang. Pessimistic bootstrapping for uncertainty-driven offline reinforcement learning. In *International Conference on Learning Representations*, 2022a.
- Yuntao Bai, Andy Jones, Kamal Ndousse, Amanda Askell, Anna Chen, Nova DasSarma, Dawn Drain, Stanislav Fort, Deep Ganguli, Tom Henighan, et al. Training a helpful and harmless assistant with reinforcement learning from human feedback. *arXiv preprint arXiv:2204.05862*, 2022b.
- Marc G Bellemare, Will Dabney, and Mark Rowland. *Distributional reinforcement learning*. MIT Press, 2023.
- Glen Berseth, Zhiwei Zhang, Grace Zhang, Chelsea Finn, and Sergey Levine. CoMPS: Continual meta policy search. *arXiv preprint arXiv:2112.04467*, 2021.
- Zhenshan Bing, David Lerch, Kai Huang, and Alois Knoll. Meta-reinforcement learning in non-stationary and dynamic environments. *IEEE Transactions on Pattern Analysis and Machine Intelligence*, 2023.
- Christopher Bishop. *Pattern Recognition and Machine Learning*. Springer, 2006.
- Paul F Christiano, Jan Leike, Tom Brown, Miljan Martic, Shane Legg, and Dario Amodei. Deep reinforcement learning from human preferences. *Advances in Neural Information Processing Systems*, 2017.
- Marc Deisenroth and Carl E Rasmussen. PILCO: A model-based and data-efficient approach to policy search. In *International Conference on Machine Learning*, 2011.
- Shibhansh Dohare, Richard S Sutton, and A Rupam Mahmood. Continual backprop: Stochastic gradient descent with persistent randomness. *arXiv preprint arXiv:2108.06325*, 2021.
- Shibhansh Dohare, Qingfeng Lan, and A. Rupam Mahmood. Overcoming policy collapse in deep reinforcement learning. In *Sixteenth European Workshop on Reinforcement Learning*, 2023.

- 
- Shibhansh Dohare, J Fernando Hernandez-Garcia, Qingfeng Lan, Parash Rahman, A Rupam Mahmood, and Richard S Sutton. Loss of plasticity in deep continual learning. *Nature*, 2024.
- Bradley Efron. *Large-scale inference: empirical Bayes methods for estimation, testing, and prediction*. Cambridge University Press, 2012.
- Scott Fujimoto, Herke Hoof, and David Meger. Addressing function approximation error in actor-critic methods. In *International Conference on Machine Learning*, 2018.
- Junyu Gao, Mengyuan Chen, Liangyu Xiang, and Changsheng Xu. A comprehensive survey on evidential deep learning and its applications. *arXiv preprint arXiv:2409.04720*, 2024.
- Andrew Gelman, John B. Carlin, Hal S. Stern, David B. Dunson, Aki Vehtari, and Donald B. Rubin. *Bayesian Data Analysis*. Chapman and Hall/CRC, 2013.
- Mohammad Ghavamzadeh, Shie Mannor, Joelle Pineau, Aviv Tamar, et al. Bayesian reinforcement learning: A survey. *Foundations and Trends® in Machine Learning*, 2015.
- Tuomas Haarnoja, Aurick Zhou, Kristian Hartikainen, George Tucker, Sehoon Ha, Jie Tan, Vikash Kumar, Henry Zhu, Abhishek Gupta, Pieter Abbeel, et al. Soft actor-critic algorithms and applications. *arXiv preprint arXiv:1812.05905*, 2018.
- Raia Hadsell, Dushyant Rao, Andrei A. Rusu, and Razvan Pascanu. Embracing change: Continual learning in deep neural networks. *Trends in Cognitive Sciences*, 2020.
- Ying Jin, Zhuoran Yang, and Zhaoran Wang. Is pessimism provably efficient for offline RL? In *International Conference on Machine Learning*, 2021.
- Sham Kakade and John Langford. Approximately optimal approximate reinforcement learning. In *International Conference on Machine Learning*, 2002.
- Christos Kaplanis, Murray Shanahan, and Claudia Clopath. Policy consolidation for continual reinforcement learning. In *International Conference on Machine Learning*, 2019.
- Ramtin Keramati, Christoph Dann, Alex Tamkin, and Emma Brunskill. Being optimistic to be conservative: Quickly learning a CVaR policy. *Proceedings of the AAAI Conference on Artificial Intelligence*, 2020.
- Khimya Khetarpal, Matthew Riemer, Irina Rish, and Doina Precup. Towards continual reinforcement learning: A review and perspectives. *Journal of Artificial Intelligence Research*, 2020.
- Diederik P Kingma and Jimmy Lei Ba. Adam: A method for stochastic optimization. In *International Conference on Learning Representations*, 2015.
- James Kirkpatrick, Razvan Pascanu, Neil Rabinowitz, Joel Veness, Guillaume Desjardins, Andrei A Rusu, Kieran Milan, John Quan, Tiago Ramalho, Agnieszka Grabska-Barwinska, et al. Overcoming catastrophic forgetting in neural networks. *Proceedings of the national academy of sciences*, 2017.
- Aviral Kumar, Rishabh Agarwal, Dibya Ghosh, and Sergey Levine. Implicit under-parameterization inhibits data-efficient deep reinforcement learning. In *International Conference on Learning Representations*, 2021.
- Saurabh Kumar, Henrik Marklund, and Benjamin Van Roy. Maintaining plasticity in continual learning via regenerative regularization. In *Proceedings of The 3rd Conference on Lifelong Learning Agents*, 2025.
- Timothy P Lillicrap, Jonathan J Hunt, Alexander Pritzel, Nicolas Heess, Tom Erez, Yuval Tassa, David Silver, and Daan Wierstra. Continuous control with deep reinforcement learning. *arXiv preprint arXiv:1509.02971*, 2015.

- 
- Guilherme Cano Lopes, Murillo Ferreira, Alexandre da Silva Simões, and Esther Luna Colombini. Intelligent control of a quadrotor with proximal policy optimization reinforcement learning. In *2018 Latin American Robotic Symposium, 2018 Brazilian Symposium on Robotics (SBR) and 2018 Workshop on Robotics in Education (WRE)*, 2018.
- Carlos E. Luis, Alessandro G. Bottero, Julia Vinogradska, Felix Berkenkamp, and Jan Peters. Value-distributional model-based reinforcement learning. *Journal of Machine Learning Research*, 2024.
- Clare Lyle, Mark Rowland, and Will Dabney. Understanding and preventing capacity loss in reinforcement learning. In *International Conference on Learning Representations*, 2022.
- Clare Lyle, Zeyu Zheng, Evgenii Nikishin, Bernardo Avila Pires, Razvan Pascanu, and Will Dabney. Understanding plasticity in neural networks. In *International Conference on Machine Learning*, 2023.
- Nis Meinert, Jakob Gawlikowski, and Alexander Lavin. The unreasonable effectiveness of deep evidential regression. In *Proceedings of the AAAI Conference on Artificial Intelligence*, 2023.
- Luckeciano Carvalho Melo and Marcos Ricardo Omena Albuquerque Máximo. Learning humanoid robot running skills through proximal policy optimization. In *2019 Latin American robotics symposium (LARS), 2019 Brazilian symposium on robotics (SBR) and 2019 workshop on robotics in education (WRE)*, 2019.
- Skander Moalla, Andrea Miele, Daniil Pyatko, Razvan Pascanu, and Caglar Gulcehre. No representation, no trust: Connecting representation, collapse, and trust issues in PPO. In *Advances in Neural Information Processing Systems*, 2024.
- Vinod Nair and Geoffrey E Hinton. Rectified linear units improve restricted Boltzmann machines. In *International Conference on Machine Learning*, 2010.
- Evgenii Nikishin, Max Schwarzer, Pierluca D’Oro, Pierre-Luc Bacon, and Aaron Courville. The primacy bias in deep reinforcement learning. In *International Conference on Machine Learning*, 2022.
- Ian Osband, Benjamin Van Roy, Daniel J Russo, and Zheng Wen. Deep exploration via randomized value functions. *Journal of Machine Learning Research*, 2019.
- Andrei A Rusu, Neil C Rabinowitz, Guillaume Desjardins, Hubert Soyer, James Kirkpatrick, Koray Kavukcuoglu, Razvan Pascanu, and Raia Hadsell. Progressive neural networks. *arXiv preprint arXiv:1606.04671*, 2016.
- John Schulman, Sergey Levine, Pieter Abbeel, Michael Jordan, and Philipp Moritz. Trust region policy optimization. In *International Conference on Machine Learning*, 2015.
- John Schulman, Philipp Moritz, Sergey Levine, Michael Jordan, and Pieter Abbeel. High-dimensional continuous control using generalized advantage estimation. *International Conference on Learning Representations*, 2016.
- John Schulman, Filip Wolski, Prafulla Dhariwal, Alec Radford, and Oleg Klimov. Proximal policy optimization algorithms. *arXiv preprint arXiv:1707.06347*, 2017.
- Murat Sensoy, Lance Kaplan, and Melih Kandemir. Evidential deep learning to quantify classification uncertainty. In S. Bengio, H. Wallach, H. Larochelle, K. Grauman, N. Cesa-Bianchi, and R. Garnett (eds.), *Advances in Neural Information Processing Systems*, 2018.
- Yihao Sun, Jiayi Zhang, Chengxing Jia, Haoxin Lin, Junyin Ye, and Yang Yu. Model-Bellman inconsistency for model-based offline reinforcement learning. In *International Conference on Machine Learning*, 2023.

- 
- Richard S. Sutton and Andrew G. Barto. *Reinforcement Learning: An Introduction*. The MIT Press, 1998.
- Emanuel Todorov, Tom Erez, and Yuval Tassa. MuJoCo: A physics engine for model-based control. In *IEEE/RSJ International Conference on Intelligent Robots and Systems*, 2012.
- Hugo Touvron, Louis Martin, Kevin Stone, Peter Albert, Amjad Almahairi, Yasmine Babaei, Nikolay Bashlykov, Soumya Batra, Prajjwal Bhargava, Shruti Bhosale, et al. Llama 2: Open foundation and fine-tuned chat models. *arXiv preprint arXiv:2307.09288*, 2023.
- René Traoré, Hugo Caselles-Dupré, Timothée Lesort, Te Sun, Guanghang Cai, Natalia Díaz-Rodríguez, and David Filliat. DisCoRL: Continual reinforcement learning via policy distillation. *arXiv preprint arXiv:1907.05855*, 2019.
- Dingrong Wang, Deep Shankar Pandey, Krishna Prasad Neupane, Zhiwei Yu, Ervine Zheng, Zhi Zheng, and Qi Yu. Deep temporal sets with evidential reinforced attentions for unique behavioral pattern discovery. In *International Conference on Machine Learning*, 2023.
- Dingrong Wang, Krishna Prasad Neupane, Ervine Zheng, and Qi Yu. Evidential conservative Q-learning for dynamic recommendations, 2024.
- R. J. Williams. Simple statistical gradient-following algorithms for connectionist reinforcement learning. *Machine Learning*, 1992.
- Hongzheng Yang, Cheng Chen, Yueyao Chen, Markus Scheppach, Hon Chi Yip, and Qi Dou. Uncertainty estimation for safety-critical scene segmentation via fine-grained reward maximization. In *Advances in Neural Information Processing Systems*, 2024.
- Tianhe Yu, Garrett Thomas, Lantao Yu, Stefano Ermon, James Y Zou, Sergey Levine, Chelsea Finn, and Tengyu Ma. MOPO: Model-based offline policy optimization. In *Advances in Neural Information Processing Systems*, 2020.
- Xujiang Zhao, Shu Hu, Jin-Hee Cho, and Feng Chen. Uncertainty-based decision making using deep reinforcement learning. In *2019 22th International Conference on Information Fusion (FUSION)*, 2019.
- Rui Zheng, Shihan Dou, Songyang Gao, Yuan Hua, Wei Shen, Binghai Wang, Yan Liu, Senjie Jin, Qin Liu, Yuhao Zhou, et al. Secrets of RLHF in large language models part i: PPO. *arXiv preprint arXiv:2307.04964*, 2023.

---

# Supplementary Materials

---

## 6 Derivations

### 6.1 Derivations for Evidential Deep Learning

We follow the derivations from [Amini et al. \(2020\)](#), adapting them to our notation whenever necessary.

**Normal Inverse-Gamma ( $\mathcal{NIG}$ ) distribution** We use the notation

$$\begin{aligned}
 (\mu, \sigma^2) | \mathbf{m} &\sim \mathcal{NIG}(\mu, \sigma^2 | \omega, \nu, \alpha, \beta) \\
 &= \mathcal{N}(\mu | \omega, \sigma^2 \nu^{-1}) \mathcal{InvGam}(\sigma^2 | \alpha, \beta) \\
 &= \frac{\beta^\alpha \sqrt{\nu}}{\Gamma(\alpha) \sqrt{2\pi\sigma^2}} \left(\frac{1}{\sigma^2}\right)^{\alpha+1} \exp\left(-\frac{2\beta + \nu(\omega - \mu)^2}{2\sigma^2}\right),
 \end{aligned}$$

where  $\omega \in \mathbb{R}$  and  $\lambda, \alpha, \beta > 0$ . The mean, mode, and variance are given by

$$\mathbb{E}[\mu] = \omega, \quad \mathbb{E}[\sigma^2] = \frac{\beta}{\alpha - 1}, \quad \text{var}[\mu] = \frac{\beta}{\nu(\alpha - 1)}, \quad \text{for } \alpha > 1.$$

The second and third terms respectively correspond to aleatoric and epistemic uncertainty.

**Model Evidence and Type II Maximum Likelihood Loss** We derive the model evidence of a  $\mathcal{NIG}$  distribution. We marginalize out  $\mu$  and  $\sigma$ :

$$\begin{aligned}
 p(y | \mathbf{m}) &= \int_{(\mu, \sigma^2)} p(y | \mu, \sigma^2) p(\mu, \sigma^2 | \mathbf{m}) d(\mu, \sigma^2) \\
 &= \int_{\sigma^2=0}^{\infty} \int_{\mu=-\infty}^{\infty} p(y | \mu, \sigma^2) p(\mu, \sigma^2 | \mathbf{m}) d\mu d\sigma^2 \\
 &= \int_{\sigma^2=0}^{\infty} \int_{\mu=-\infty}^{\infty} p(y | \mu, \sigma^2) p(\mu, \sigma^2 | \omega, \nu, \alpha, \beta) d\mu d\sigma^2 \\
 &= \int_{\sigma^2=0}^{\infty} \int_{\mu=-\infty}^{\infty} \left[ \sqrt{\frac{1}{2\pi\sigma^2}} \exp\left(-\frac{(y - \mu)^2}{2\sigma^2}\right) \right] \\
 &\quad \left[ \frac{\beta^\alpha \sqrt{\nu}}{\Gamma(\alpha) \sqrt{2\pi\sigma^2}} \left(\frac{1}{\sigma^2}\right)^{\alpha+1} \exp\left(-\frac{2\beta + \nu(\omega - \mu)^2}{2\sigma^2}\right) \right] d\mu d\sigma^2 \\
 &= \int_{\sigma^2=0}^{\infty} \frac{\beta^\alpha \sigma^{-3-2\alpha}}{\sqrt{2\pi} \sqrt{1 + 1/\nu} \Gamma(\alpha)} \exp\left(-\frac{2\beta + \frac{\nu(y - \omega)^2}{1 + \nu}}{2\sigma^2}\right) d\sigma^2 \\
 &= \int_{\sigma=0}^{\infty} \frac{\beta^\alpha \sigma^{-3-2\alpha}}{\sqrt{2\pi} \sqrt{1 + 1/\nu} \Gamma(\alpha)} \exp\left(-\frac{2\beta + \frac{\nu(y - \omega)^2}{1 + \nu}}{2\sigma^2}\right) 2\sigma d\sigma \\
 &= \frac{\Gamma(1/2 + \alpha)}{\Gamma(\alpha)} \sqrt{\frac{\nu}{\pi}} (2\beta(1 + \nu))^\alpha \left(\nu(y - \omega)^2 + 2\beta(1 + \nu)\right)^{-(\frac{1}{2} + \alpha)},
 \end{aligned}$$

where  $\Gamma(\cdot)$  is the Gamma function. Therefore, we have that the evidence distribution  $p(y | \mathbf{m})$  is a Student-t distribution, i.e.,

$$p(y | \mathbf{m}) = \text{St}\left(y | \omega, \frac{\beta(1 - \nu)}{\nu\alpha}, 2\alpha\right),$$

which is evaluated at  $y$  with location parameter  $\omega$ , scale parameter  $\beta(1 - \nu)/\nu\alpha$ , and degrees of freedom  $2\alpha$ . We can compute the negative log-likelihood (NLL) loss as:

$$\begin{aligned}\mathcal{L}_{\text{NLL}}(\mathbf{m}) &= -\log p(y|\mathbf{m}) \\ &= -\log \left( \text{St} \left( y \middle| \omega, \frac{\beta(1 - \lambda)}{\nu\alpha}, 2\alpha \right) \right) \\ &= \frac{1}{2} \log \left( \frac{\pi}{\nu} \right) - \alpha \log(\Omega) + \left( \alpha + \frac{1}{2} \right) \log \left( (y - \omega)^2 \nu + \Omega \right) + \log \left( \frac{\Gamma(\alpha)}{\Gamma(\alpha + \frac{1}{2})} \right)\end{aligned}$$

where  $\Omega = 2\beta(1 + \nu)$ .

## 6.2 Derivations for the Generalized Advantage Estimator

Given the definition of the  $k$ -step estimator as  $\hat{A}_t^{(k)} = -V_t + \gamma^k V_{t+k} + \sum_{l=0}^{k-1} \gamma^l r_{t+l}$ , we have that

$$\text{var} \left[ \hat{A}_t^{(k)} \right] = \text{var} [V_t] + \gamma^{2k} \text{var} [V_{t+k}].$$

We adapt our estimator’s variance approximation for EPPO<sub>ind</sub> to

$$\begin{aligned}\text{var} \left[ \hat{A}_t^{\text{GAE}} \right] &\approx (1 - \lambda)^2 \sum_{l=1}^{\infty} \lambda^{2(l-1)} \text{var} \left[ \hat{A}_t^{(l)} \right] \\ &= (1 - \lambda)^2 \left( \text{var} [V_t] \sum_{l=0}^{\infty} \lambda^{2l} + \sum_{l=1}^{\infty} \gamma^{2l} \lambda^{2(l-1)} \text{var} [V_{t+l}] \right) \\ &= \frac{(1 - \lambda)^2}{1 - \lambda^2} \text{var} [V_t] + \left( \frac{1 - \lambda}{\lambda} \right)^2 \sum_{l=1}^{\infty} (\gamma\lambda)^{2l} \text{var} [V_{t+l}],\end{aligned}$$

i.e., the form we have in (5).

## 7 Further Details on Experiments

### 7.1 Experiment Details

In this section, we outline the details and design choices for our experiments and non-stationary environments. We use the `Ant` and `HalfCheetah` environments with the ‘v5’ versions of MuJoCo (Todorov et al., 2012), as these tasks are stable and do not reward the agent for maintaining stability.

#### 7.1.1 Slippery Environments

Our experimental design is inspired by Dohare et al. (2021; 2024). We construct a non-stationary environment by varying the floor’s friction coefficient. Searching for feasible friction values we set the minimum at 0.5 and the maximum at 4.0. Outside of this range, solving the tasks either become infeasible or yield low rewards due to excessive action costs, limited movement, or the agent simply falling.

To introduce variation across tasks while ensuring differences between tasks, we incrementally change the friction by 0.25, resulting in 15 distinct tasks. We implement two strategies for these changes:

- `decreasing`: Friction starts at its maximum value and gradually decreases.
- `increasing`: Friction starts at its minimum value and gradually increases.



---

These setups ensures that the agents experience non-stationarity in both increasing and decreasing friction scenarios. We implement these changes by modifying the publicly available environment XML files<sup>2 3</sup> to adjust the floor friction coefficients.

### 7.1.2 Paralysis Environments

We introduce a novel set of non-stationarity experiments by dynamically modifying the torque capabilities of leg joints in the `Ant` and `HalfCheetah` environments, inspired by [Al-Shedivat et al. \(2018\)](#). Specifically, we define six torque modification schemes for `Ant` and four for `HalfCheetah`. Each scheme targets selected joints, progressively reducing their torque capacity until they become completely paralyzed, after which their functionality is gradually restored to the fully operational state. This process results in a sequence of nine tasks, where each joint’s torque capacity changes in increments of 25%, following the pattern: [100, 75, 50, 25, 0, 25, 50, 75, 100]. Note that while the policy can still output full torques, the applied torque is scaled according to the specified coefficients.

**Paralysis on Ant.** The `Ant` environment consists of four legs and eight joints. We design distinct experiments by paralyzing different joints, ensuring that control tasks remain unique across experiments. For instance, if we paralyze the right back leg, we do not conduct a separate experiment on the left back leg, as the locomotion is symmetric and would result in an equivalent control task. We create the following experiments:

- `back-one`: Paralyzing a single back leg. The affected joints are 6 and 7.
- `front-one`: Paralyzing a single front leg. The affected joints are 2 and 3.
- `back-two`: Paralyzing both back legs. The affected joints are 0, 1, 6, and 7.
- `front-two`: Paralyzing both front legs. The affected joints are 2, 3, 4, and 5.
- `cross`: Paralyzing diagonally opposite legs (right back and left front). The affected joints are 0, 1, 2, and 3.
- `parallel`: Paralyzing the left-side legs (one back and one front). The affected joints are 2, 3, 6, and 7.

**Paralysis on HalfCheetah.** The `HalfCheetah` environment consists of two legs and four joints. To prevent the agent from resorting to crawling, we modify only one joint per leg. We create the following experiments:

- `back-one`: Paralyzing a single joint in the back leg. The affected joint is 2.
- `front-one`: Paralyzing a single joint in the front leg. The affected joint is 5.
- `cross-v1`: Paralyzing diagonally opposite joints in the back and front legs. The affected joints are 2 and 4.
- `cross-v2`: Paralyzing a different pair of diagonally opposite joints in the back and front legs. The affected joints are 1 and 5.

## 7.2 Hyperparameters

In this section, we provide all the necessary details to reproduce EPPO. We evaluate EPPO with ten repetitions using the following seeds: [1, 2, 3, 4, 5, 6, 7, 8, 9, 10]. We list the hyperparameters for the experimental pipeline in Table 2.

---

<sup>2</sup><https://github.com/Farama-Foundation/Gymnasium/blob/main/gymnasium/envs/mujoco/assets/ant.xml>

<sup>3</sup>[https://github.com/Farama-Foundation/Gymnasium/blob/main/gymnasium/envs/mujoco/assets/half\\_cheetah.xml](https://github.com/Farama-Foundation/Gymnasium/blob/main/gymnasium/envs/mujoco/assets/half_cheetah.xml)

Table 2: Common hyperparameters used in the experimental pipeline.

Policy learning	
Seeds	[1, 2, 3, 4, 5, 6, 7, 8, 9, 10]
Number of steps per task	500 000
Learning rate for actor	0.0003
Learning rate for critic	0.0003
Horizon	2048
Number of epochs	10
Minibatch size	256
Clip rate $\epsilon$	0.2
GAE parameter $\lambda$	0.95
Hidden dimensions of actor	[256, 256]
Hidden dimensions of critic	[256, 256]
Activation functions of actor	ReLU
Activation functions of critic	ReLU
Normalization layers of actor	Layer Norm
Normalization layers of critic	Layer Norm
Discount factor $\gamma$	0.99
Maximum gradient norm	0.5
Evaluation-related	
Evaluation frequency (steps)	20 000 and end of the tasks
Evaluation episodes	10
EPP0-related	
Regularization coefficient ( $\xi$ )	0.01
Hyperprior distribution of $w$	$\mathcal{N}(w 0, 100^2)$
Hyperprior distribution of $\nu$	$\mathcal{Gam}(\nu 5, 1)$
Hyperprior distribution of $\alpha$	$\mathcal{Gam}(\alpha 5, 1) + 1^\dagger$
Hyperprior distribution of $\beta$	$\mathcal{Gam}(\beta 5, 1)$
Grid Search-related	
Seeds	[1001, 1002, 1003]
Radius parameter $\kappa$ for EPP0 <sub>cor</sub>	[0.01, 0.1, 0.25]
Radius parameter $\kappa$ for EPP0 <sub>ind</sub>	[0.01, 0.05, 0.1]

<sup>†</sup>The +1 ensures a finite mean for  $\alpha$ .

Table 3: Radius parameters ( $\kappa$ ) of EPPO.

Experiment	Environment	Strategy	Confidence radius parameter ( $\kappa$ )	
			EPPO <sub>cor</sub>	EPPO <sub>ind</sub>
Slippery	Ant	decreasing	0.05	0.1
		increasing	0.1	0.25
	HalfCheetah	decreasing	0.05	0.1
		increasing	0.1	0.1
Paralysis	Ant	back-one	0.05	0.01
		front-one	0.1	0.1
		back-two	0.01	0.25
		front-two	0.1	0.01
		cross	0.01	0.1
		parallel	0.05	0.01
	HalfCheetah	back-one	0.05	0.01
		front-one	0.1	0.1
		cross-v1	0.05	0.25
		cross-v2	0.05	0.1

### 7.2.1 Training

**Architecture and Optimization Details.** We train EPPO for 500 000 steps per task, performing updates to the policy and critic 10 times every 2048 step with a batch size of 256. The learning rate is set to 0.0003 for both the actor and critic, optimized using Adam (Kingma & Ba, 2015). The actor and critic networks each consist of a 2-layer feedforward neural network with 256 hidden units. Unlike other baselines, our critic network outputs four values instead of one to predict the evidential priors. We apply Layer Normalization (Ba et al., 2016) and ReLU activations (Nair & Hinton, 2010) for both networks. The policy follows a diagonal normal distribution. Following common practice in the literature, we set the discount factor to  $\gamma = 0.99$ , the GAE parameter to  $\lambda = 0.95$ , and the clipping rate to  $\epsilon = 0.2$ . Gradient norms are clipped at 0.5, and GAE advantage estimates are normalized within each batch.

**Evaluation Details.** We evaluate the models at the beginning and final steps of each task, as well as every 20 000 steps, using 10 evaluation episodes. The evaluation environment seeds are set to the training seed plus 100. For metric calculation, we use the mean return across the evaluation episodes.

**EPPO Details.** We set the regularization coefficient ( $\xi$ ) to 0.01 to scale it down, selecting this value heuristically based on its contribution to the total loss. To prevent overfitting and allow flexibility in learning, we use uninformative, flat priors for the hyperprior distributions. Specifically, we choose a normal distribution  $\mathcal{N}(\omega|0, 100^2)$  for  $\omega$ , though a positively skewed distribution may further improve performance. For  $\nu$ ,  $\alpha$ , and  $\beta$ , we use a gamma distribution  $\mathcal{Gam}(5, 1)$  to ensure positivity. Additionally, we shift the hyperprior distribution of  $\alpha$  by +1 to ensure a finite mean.

**EPPO Optimism Grid Search Details.** We introduce a confidence radius parameter ( $\kappa$ ) that controls the level of optimism incorporated into exploration. To determine an appropriate value, we perform a grid search over  $\kappa \in [0.01, 0.05, 0.1]$  for EPPO<sub>ind</sub> and  $\kappa \in [0.01, 0.1, 0.25]$  for EPPO<sub>cor</sub>, selecting these ranges based on their influence on the advantage estimate. We train models using three seeds (1001, 1002, 1003) and exclude them from the main results. After evaluating the AULC metric, we select the optimal  $\kappa$  values and use them for EPPO’s final evaluation. Table 3 presents  $\kappa$  values selected for the training.

Table 4: *Performance evaluation on the slippery environments.* Area Under the Learning Curve (AULC) and Final Return (mean $\pm$ se) scores are averaged over ten repetitions. The highest mean values are highlighted in bold and underlined if they fall within one standard error of the best score. The average score represents the mean across all environments, while the average ranking is determined based on the ranking of the mean scores.

Metric	Model	decreasing		increasing		Average	
		Ant	HalfCheetah	Ant	HalfCheetah	Score	Ranking
AULC ( $\uparrow$ )	PPO	2114 $\pm$ 260	<u>2631<math>\pm</math>225</u>	2117 $\pm$ 363	2702 $\pm$ 338	2391	4.3
	PFO	<u>2456<math>\pm</math>113</u>	2216 $\pm$ 201	2522 $\pm$ 96	1830 $\pm$ 551	2256	3.8
	EPPO <sub>mean</sub>	<u>2420<math>\pm</math>164</u>	2157 $\pm$ 402	<u>2854<math>\pm</math>111</u>	2913 $\pm$ 288	2586	3.5
	EPPO <sub>cor</sub>	2374 $\pm$ 142	<u>2818<math>\pm</math>306</u>	<b>2907<math>\pm</math>98</b>	<b>3829<math>\pm</math>241</b>	<b>2982</b>	2.0
	EPPO <sub>ind</sub>	<b>2549<math>\pm</math>170</b>	<b>2861<math>\pm</math>308</b>	<u>2879<math>\pm</math>78</u>	3386 $\pm$ 217	2919	<b>1.5</b>
FINAL RETURN ( $\uparrow$ )	PPO	2079 $\pm$ 290	2577 $\pm$ 241	2223 $\pm$ 383	2913 $\pm$ 349	2448	4.3
	PFO	<u>2528<math>\pm</math>111</u>	2240 $\pm$ 223	2647 $\pm$ 104	1931 $\pm$ 592	2336	4.3
	EPPO <sub>mean</sub>	<u>2583<math>\pm</math>172</u>	2217 $\pm$ 443	<u>2975<math>\pm</math>133</u>	3055 $\pm$ 299	2707	3.3
	EPPO <sub>cor</sub>	<u>2538<math>\pm</math>146</u>	<u>2935<math>\pm</math>318</u>	<b>3047<math>\pm</math>109</b>	<b>4081<math>\pm</math>236</b>	<b>3150</b>	1.8
	EPPO <sub>ind</sub>	<b>2691<math>\pm</math>180</b>	<b>2953<math>\pm</math>322</b>	<u>3045<math>\pm</math>80</u>	3572 $\pm$ 216	3065	<b>1.5</b>

### 7.3 Results Tables and Visualizations

We present the detailed results of the experiments in Table 4 and Table 5. The learning curves across environment steps are illustrated in Figures 3 to 5. In these figures, the thick (dashed/dotted/dash-dotted/solid) curve represents the mean returns across ten evaluation episodes and ten random seeds, with the shaded area indicating one standard error from the mean. The legend provides the mean and standard error for the AULC and final return scores, listed in this order. The vertical black dotted lines mark the task changes.

Table 5: *Performance evaluation on the paralysis environments.* Area Under the Learning Curve (AULC) and Final Return (mean $\pm$ se) scores are averaged over ten repetitions. The highest mean values are highlighted in bold and underlined if they fall within one standard error of the best score. The average score represents the mean across all environments, while the average ranking is determined based on the ranking of the mean scores.

Metric	Environment	Strategy	Model				
			PPO	PFO	EPPO <sub>mean</sub>	EPPO <sub>cor</sub>	EPPO <sub>ind</sub>
AULC ( $\uparrow$ )	Ant	back-one	2286 $\pm$ 258	2141 $\pm$ 118	<u>2498<math>\pm</math>95</u>	<u>2522<math>\pm</math>154</u>	<b>2707<math>\pm</math>219</b>
		front-one	2426 $\pm$ 136	2102 $\pm$ 83	2506 $\pm$ 115	<b>2884<math>\pm</math>122</b>	<u>2715<math>\pm</math>162</u>
		back-two	2090 $\pm$ 103	<u>2130<math>\pm</math>71</u>	<b>2179<math>\pm</math>99</b>	2058 $\pm$ 84	1947 $\pm$ 80
		front-two	2165 $\pm$ 96	1979 $\pm$ 59	<u>2325<math>\pm</math>118</u>	<b>2328<math>\pm</math>126</b>	<u>2289<math>\pm</math>104</u>
		parallel	2417 $\pm$ 147	2291 $\pm$ 110	2261 $\pm$ 122	2214 $\pm$ 140	<b>2524<math>\pm</math>204</b>
		cross	2125 $\pm$ 82	2166 $\pm$ 82	<u>2227<math>\pm</math>110</u>	<u>2271<math>\pm</math>86</u>	<b>2287<math>\pm</math>90</b>
	Average AULC on Ant		2252	2135	2333	2380	<b>2411</b>
	HalfCheetah	back-one	2246 $\pm$ 257	1792 $\pm$ 323	2952 $\pm$ 355	<u>3464<math>\pm</math>240</u>	<b>3465<math>\pm</math>189</b>
		front-one	1836 $\pm$ 327	2279 $\pm$ 339	3319 $\pm$ 298	<u>3509<math>\pm</math>303</u>	<b>3726<math>\pm</math>330</b>
		cross-v1	2165 $\pm$ 301	2168 $\pm$ 400	<u>2941<math>\pm</math>322</u>	<b>3221<math>\pm</math>313</b>	3110 $\pm$ 287
		cross-v2	2233 $\pm$ 275	1774 $\pm$ 290	3021 $\pm$ 262	<u>3161<math>\pm</math>260</u>	<b>3348<math>\pm</math>272</b>
		Average AULC on HalfCheetah		2120	2003	3058	3339
	Overall Average AULC Score			2199	2082	2623	2763
Overall Average Ranking on AULC			4.0	4.2	2.8	2.2	<b>1.8</b>
FINAL RETURN ( $\uparrow$ )	Ant	back-one	2587 $\pm$ 249	2372 $\pm$ 110	<u>2738<math>\pm</math>107</u>	<u>2787<math>\pm</math>149</u>	<b>2951<math>\pm</math>211</b>
		front-one	2668 $\pm$ 156	2324 $\pm$ 76	2713 $\pm$ 129	<b>3117<math>\pm</math>120</b>	2934 $\pm$ 188
		back-two	<u>2393<math>\pm</math>111</u>	<u>2438<math>\pm</math>85</u>	<b>2486<math>\pm</math>119</b>	2361 $\pm$ 90	2164 $\pm$ 97
		front-two	2482 $\pm$ 115	2222 $\pm$ 62	<u>2621<math>\pm</math>129</u>	<b>2653<math>\pm</math>124</b>	<u>2615<math>\pm</math>127</u>
		parallel	<u>2686<math>\pm</math>146</u>	2616 $\pm$ 120	2572 $\pm$ 137	2486 $\pm$ 159	<b>2846<math>\pm</math>204</b>
		cross	2411 $\pm$ 107	<u>2475<math>\pm</math>92</u>	<u>2532<math>\pm</math>124</u>	<u>2563<math>\pm</math>91</u>	<b>2564<math>\pm</math>97</b>
	Average Final Return on Ant		2538	2408	2610	2661	<b>2679</b>
	HalfCheetah	back-one	2255 $\pm$ 287	1826 $\pm$ 347	3074 $\pm$ 377	<u>3660<math>\pm</math>250</u>	<b>3675<math>\pm</math>194</b>
		front-one	1897 $\pm$ 352	2352 $\pm$ 363	3465 $\pm$ 301	<u>3680<math>\pm</math>315</u>	<b>3922<math>\pm</math>343</b>
		cross-v1	2213 $\pm$ 358	2170 $\pm$ 436	3087 $\pm$ 339	<b>3434<math>\pm</math>326</b>	<u>3336<math>\pm</math>305</u>
		cross-v2	2264 $\pm$ 290	1768 $\pm$ 310	3198 $\pm$ 267	<u>3365<math>\pm</math>269</u>	<b>3536<math>\pm</math>290</b>
	Average Final Return on HalfCheetah		2157	2029	3206	3535	<b>3617</b>
	Overall Average Final Return Score			2386	2256	2849	3011
Overall Average Ranking on Final Return			3.9	4.3	2.8	2.2	<b>1.8</b>

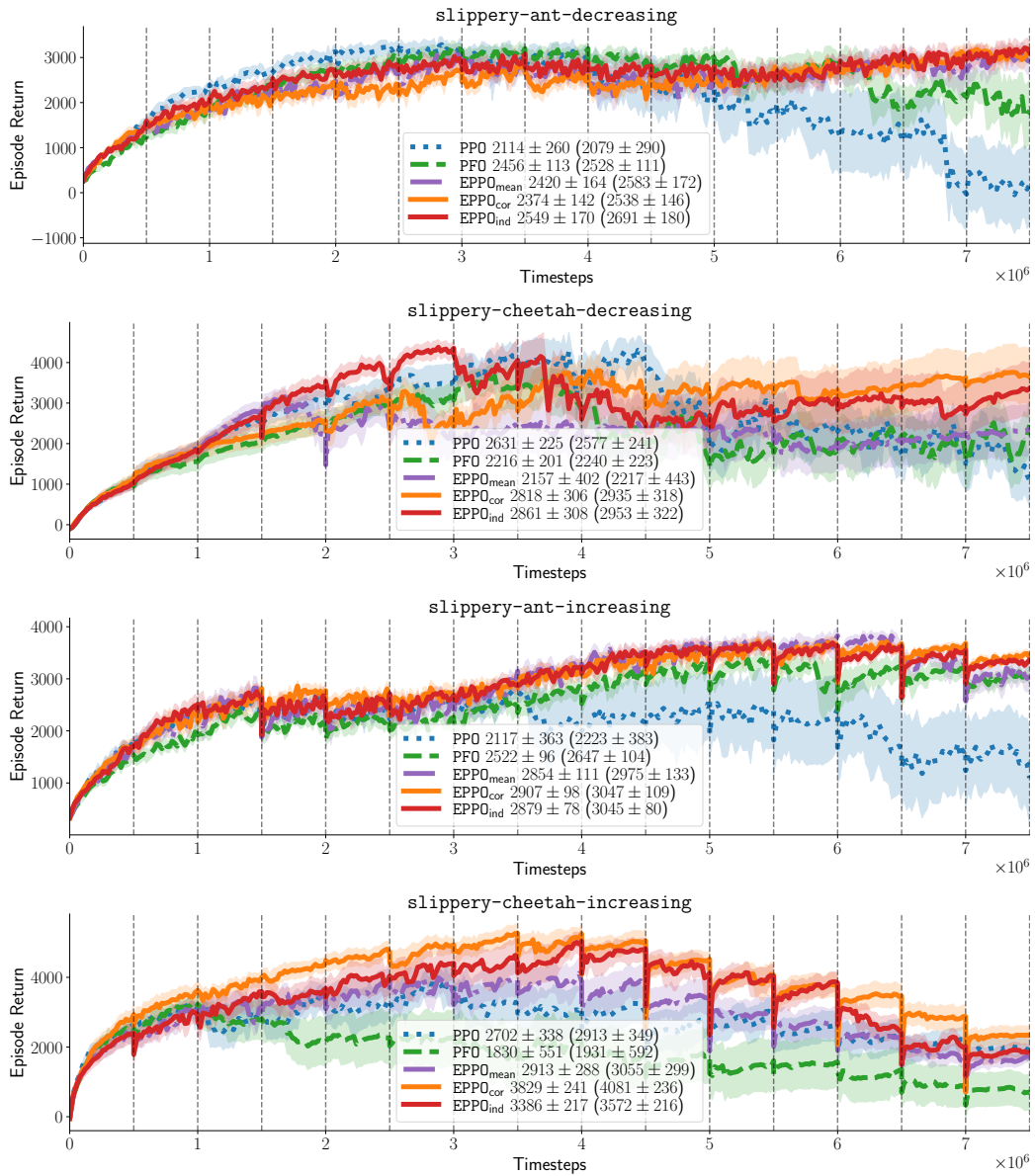


Figure 3: Learning curves for the slippery experiment.



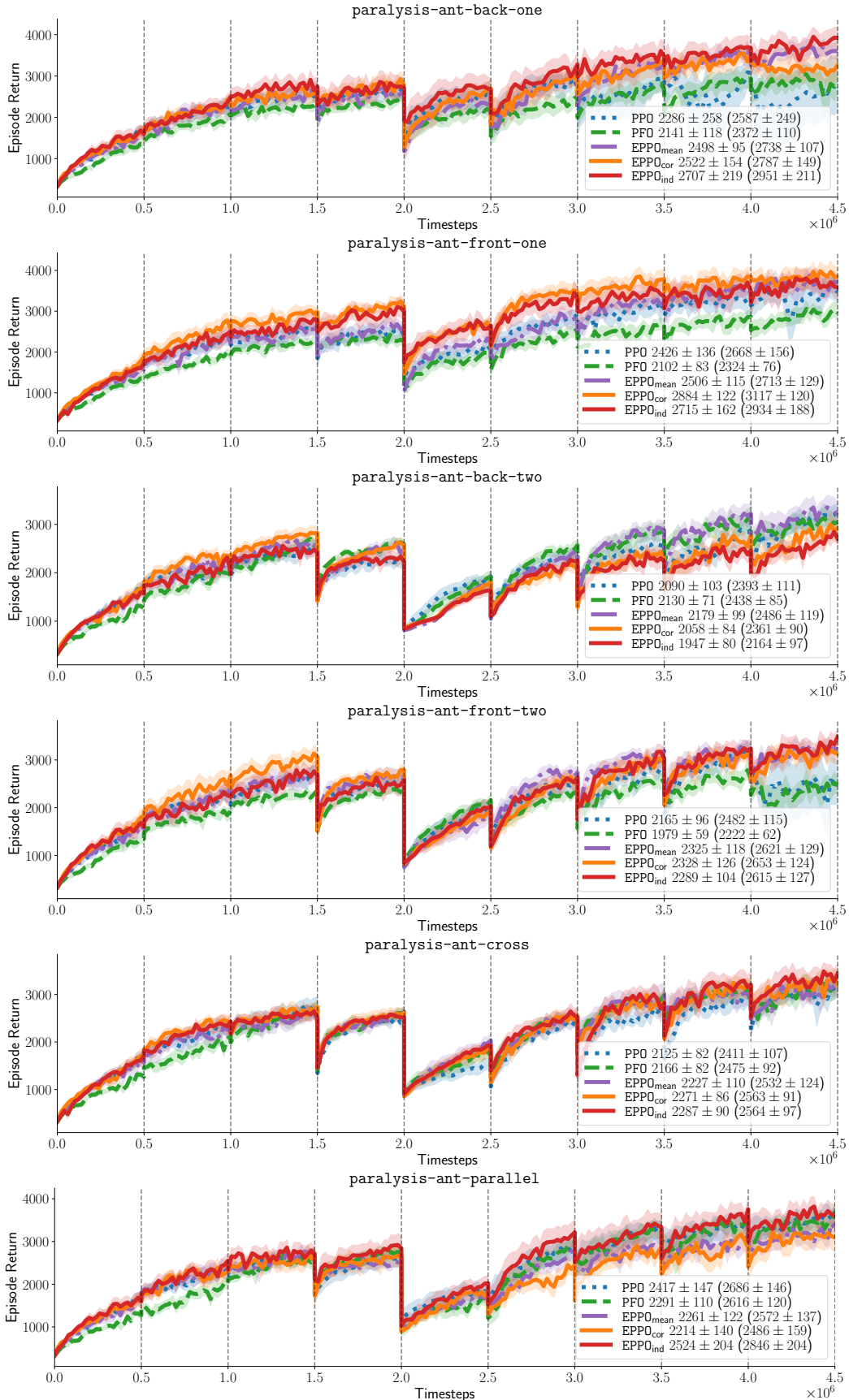


Figure 4: Learning curves for the paralysis experiment on Ant environment.

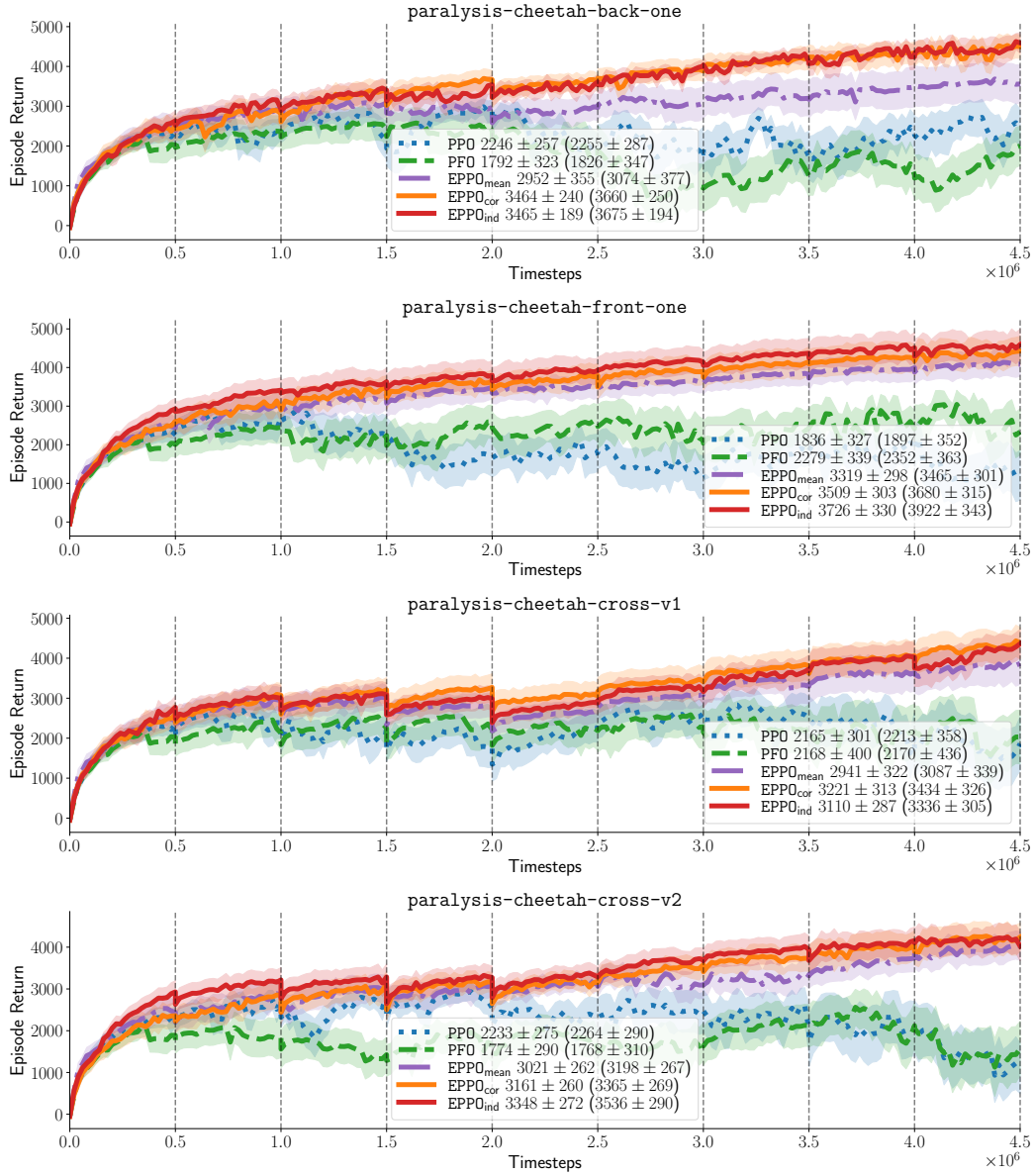


Figure 5: Learning curves for the paralysis experiment on HalfCheetah environment.